

Multi-Sensor Frequency Domain Multiple Access Interference Canceller for DS-CDMA Systems

Luis Gonçalves^{1,3}, Atílio Gameiro^{2,3}

¹Departamento de Matemáticas e Engenharias, Universidade da Madeira, Portugal

²Departamento de Electrónica e Telecomunicações, Universidade de Aveiro, Portugal

³Instituto de Telecomunicações, Campus Universitário de Santiago, 3810-193 Aveiro, Portugal

email: luisgo@uma.pt, amg@det.ua.pt

DOI Link: <http://doi.wiley.com/10.1002/ett.1146>

Abstract

Direct Sequence Code Division Multiple Access (DS-CDMA) signals exhibit cyclostationary properties which imply redundancy between frequency components separated by multiples of the symbol rate. In this paper a Multiple Access Interference (MAI) Canceller (Frequency Shift Canceller (FSC)) that explores this property is presented. The linear frequency domain canceller operates on the spreaded signal so as to minimise the interference and noise at the output (Minimum Mean Squared Error Criterium). The performance of multi-sensor configurations for the cases of beamforming and uncorrelated spatial channels was evaluated considering both synchronous (UMTS-TDD) and time misalignment systems. The FSC configurations were concatenated with 2D-PIC structure and evaluated. The simulation results show considerable improvement relative to the conventional 2D-RAKE and 2D-PIC receiver. A performance close to the single-user RAKE case was achieved when it was evaluated jointly with 2D-PIC.

1 Introduction

Direct sequence Code Division Multiple Access (DS-CDMA) has emerged as one of the most promising techniques to implement various radio communication systems. It presents significant advantages over Time Division Multiple Access (TDMA), in terms of its adoption, frequency diversity, multipath diversity and enhanced spectrum efficiency in multi-cell systems [1], which led as the candidate choice for third generation cellular systems. The first version of third generation CDMA systems is based on the conventional RAKE receiver, which is known to be limited by multiple access interference (MAI) and requires very precise power control. To overcome these limitations, joint detection of the received DS-CDMA signals has been proposed at the base station (BS) or at the user equipment. The optimum joint detector [2], although well known, results in prohibitively high computational complexity, and consequently effort has been made to devise suboptimum algorithms [3–7] with good tradeoff between performance and complexity that can be implemented at low cost in future CDMA systems. In this paper, we propose a low complexity MAI canceller whose approach can be considered a feasible solution for broadband DS-CDMA signals.

A DS-SS signal is a particular case of a random pulse amplitude modulation. It is well known [8] that these signals exhibit cyclostationary properties which imply redundancy (diversity) between frequency components separated by multiples of the symbol rate. This characteristic is explored in the proposed MAI canceller, named hereafter as the Frequency Shift Canceller (FSC) detector.

The canceller fits in the category of frequency shift (FRESH) filters [9] which are structures that use the correlation between bands inherent in most man made signals. The use of FRESH filters has been proposed for signal extraction of Multi-user Direct Sequence signals [10, 11].

Most of the work on such type of structures reported in the literature follows a time domain approach. In this paper, we explore the correlation between frequency bands to remove the MAI in Multi-user Direct Spread Spectrum Signals, but in terms of implementation consider a frequency domain approach, and extend the algorithm to situations where signals with different code lengths coexist. The frequency domain approach enables digital implementation using fast fourier transform (FFT) modules, allowing significant complexity savings, while the generalisation to variable length spreading codes allows direct application of the canceller with UMTS systems. Approximately the complexity of the algorithm per user and antenna requires the inversion of an Hermitian Definite positive matrix per symbol. The size of the matrix is equal to the number of redundant frequency bands considered and must be at least equal to the number of users if perfect signal extraction is to be achieved in the absence of noise. Considering noise, the performance can be improved by using a higher number of frequency bands, whose maximum number depends on the code length and excess bandwidth of the pulse shaping filter. Currently the implementation of real time matrix inversion is not a constrain in the advent of specific ASIC processors that accelerates this function.

It is consensual that the use of antenna arrays is a key component to increase the capacity cellular systems [12, 13]. The performance and complexity of a multi-sensor detector is dependent on the array/multipath processing and multi-user detection units [14] and therefore we investigate several array processing configurations for the multi-sensor FSC, and consider the cases of high correlation between antenna elements channels (beamforming) and low correlation (diversity).

The paper is outlined as follows: in Section 2 we present the theoretical framework and show that in a DS-SS signal non-overlapping frequency bands separated by a multiple of the baud rate are linearly related; in Section 3 the architecture and design principles of a MAI canceller are presented; in Section 4 several configurations involving the detector FSC are presented; in Section 5 simulation results are presented for a given scenario in a UMTS-TDD system and in a time misalignment system; Finally in Section 6 the main conclusions of this work are outlined.

2 Theoretical Background

A DS-SS signal is represented as

$$s(t) = \sum_k a_k g(t - kT) \quad (1)$$

where $\{a_k\}$ is the sequence of information symbols, $\frac{1}{T}$ the symbol rate and $g(t)$ is the signature waveform, which assuming a spreading factor Q_{max} can be written as

$$g(t) = \sum_{q=0}^{Q_{max}-1} c_h p(t - qT_c) * h(t) \quad (2)$$

where $\{c_h\}$ is the code sequence, $p(t)$ the normalized elementary pulse, T_c the chip period, $h(t)$ is a linear filter that may represent a channel impulse response and the symbol $*$ stands for convolution.

The Fourier Transform of $s(t)$ is

$$S(f) = \sum_k a_k G(f) e^{-j2\pi f k T} = G(f) A(f) \quad (3)$$

with

$$\begin{aligned} A(f) &= \sum_k a_k e^{-j2\pi f k T} \\ G(f) &= P(f) H(f) \sum_{v=0}^{Q_{max}-1} c_v e^{-j2\pi f v T_c} \end{aligned} \quad (4)$$

From (4) it is easy to verify that

$$A(f + \frac{i}{T}) = A(f) \quad \forall i \in \mathbb{Z} \quad (5)$$

Assuming that the elementary pulse $p(t)$ has a bilateral bandwidth $\frac{\alpha}{T_c}$, where typically (for pulse of the raised cosine family) α is a number between one and two, we can say that the signal bandwidth is $\frac{\alpha Q_{max}}{T}$ *i.e.* from (5) we have a αQ_{max} order frequency diversity.

Let us define

$$\begin{aligned} S_{mB}(f) &= S\left(f + \frac{m}{T}\right) \text{rect}(fT) \\ G_{mB}(f) &= G\left(f + \frac{m}{T}\right) \text{rect}(fT) \end{aligned} \quad (6)$$

where

$$\text{rect}(f) = \begin{cases} 1 & \text{if } f \in \left[-\frac{1}{2}, \frac{1}{2}\right[\\ 0 & \text{if } f \notin \left[-\frac{1}{2}, \frac{1}{2}\right[\end{cases} \quad (7)$$

and m is the index of the band. Hereafter the subscript B means a signal frequency shifted to baseband. Then using (6) for two bands of index m_1 and m_2 and assuming $G_{m_1B}(f)$ has no singularities, it can be concluded that in the interval $f \in \left[-\frac{1}{2T}, \frac{1}{2T}\right[$ we have that

$$S_{m_2B}(f) = \frac{G_{m_2B}(f)}{G_{m_1B}(f)} S_{m_1B}(f) \quad (8)$$

that is the signal information in non-overlapping frequency bands spaced by a multiple of the baud rate are related through a linear transformation.

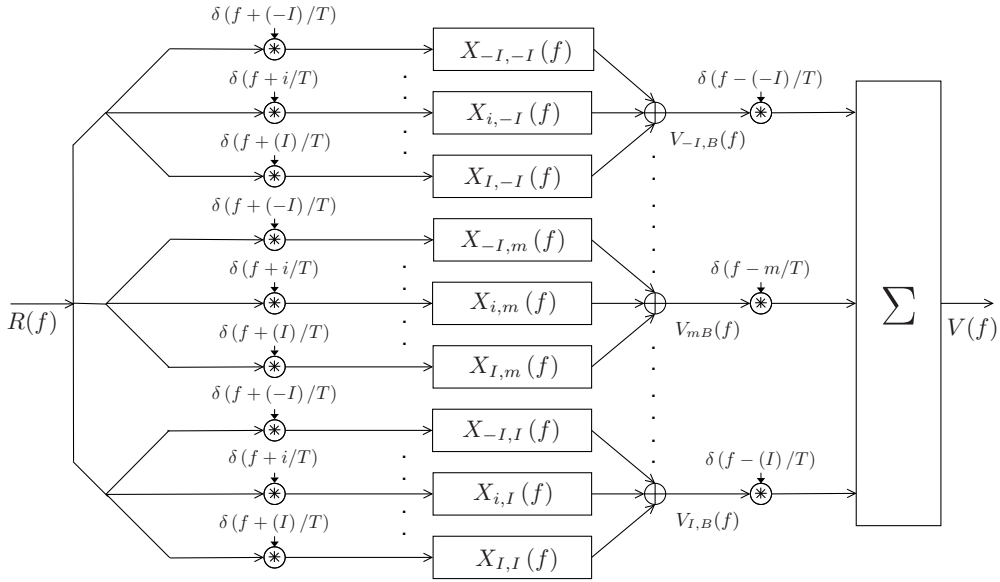


Figure 1: Conceptual Schematic of the Canceller.

3 Canceller Architecture

The canceller operates in the frequency domain but in practical implementation or simulation, the time to frequency domain conversion will be performed digitally through a FFT. However, in the derivations we shall use a continuous representation for the functions

The architecture of the canceller is shown in Figure 1, for a given user. The symbol * stands for convolution and δ is the Dirac impulse.

Assuming U users, the input signal in the frequency domain is given by

$$R(f) = \sum_{u=1}^U S^{(u)}(f) + N(f) \quad (9)$$

where $N(f)$ is the Fourier transform of the additive noise, with power spectral density $\eta_{in}(f)$ and $S^{(u)}(f)$ is the Fourier transform of $s^{(u)}(t)$ where the superscript (u) refers to the user.

In the base station where all the signals have also to be recovered, the canceller consists of the replica of this basic receiver for each user. However, it can be applied to the mobile station provided the codes for the different users are known.

We shall start by considering the case where all the users have the same spreading factor and then proceed with the generalization for multirate.

3.1 Identical Spreading Factor

Let us consider without loss of generality that user one is the user of interest. From (8) this constraint implies that the filters $X_{i,m}(f)$ be of the form

$$X_{i,m}(f) = \alpha_{i,m}(f) \frac{G_{mB}^{(1)}(f)}{G_{iB}^{(1)}(f)} \quad (10)$$

where $\alpha_{i,m}(f)$ are complex weight functions.

Using (10), the baseband shifts of the output signal $V(f)$ are given by

$$V_{mB}(f) = S_{mB}^{(1)}(f) \left(\sum_{i=-I}^I \alpha_{i,m}(f) \right) + \sum_{u=2}^U \left[\sum_k a_k^{(u)} e^{-j2\pi f k T} \beta_{mB}^{(u)}(f) \right] + N'_{mB}(f) \quad (11)$$

where $S_{mB}^{(1)}(f)$ is defined in (6) and

$$\beta_{mB}^{(u)}(f) = \sum_{i=-I}^I \alpha_{i,m}(f) \frac{G_{mB}^{(1)}(f)}{G_{iB}^{(1)}(f)} G_{iB}^{(u)}(f) \quad (12)$$

¹In case of a singularity with $G_{iB}^{(1)}(f) = 0$ for a particular $f = f_1$ then is considered $X_{i,m}(f_1) = 0$.

From (11) we conclude that the condition that the signal of interest is not distorted is verified provided $\sum_i \alpha_{i,m}(f) = \text{rect}(fT)$. The power spectral density of additive noise disturbance at the output $N'_{mB}(f)$ is given by

$$\eta_{out_{mB}}(f) = \sum_{i=-I}^I |\alpha_{i,m}(f)|^2 \left| \frac{G_{mB}^{(1)}(f)}{G_{iB}^{(1)}(f)} \right|^2 \eta_{in_{iB}}(f) \quad (13)$$

The minimization of the output overall disturbance can be achieved, minimizing the power spectral density of the error term in (11) assuming that the information data sequences $\{a_k^{(u)}\}$ are sequences of *i.i.d.* random variables with $E[a_k^{(u)}] = 0$ and $E\left[|a_k^{(u)}|^2\right] = 1$. Defining the error function as $e(f) = (V_{mB}(f) - S_{mB}^{(1)}(f))$ in (11) assuming that $\sum_i \alpha_{i,m}(f) = \text{rect}(fT)$ we get

$$C_m(f) = E\left[|e(f)|^2\right] = L_s \sum_{u=2}^U \left| \beta_{mB}^{(u)}(f) \right|^2 + \eta_{out_{mB}}(f) \quad (14)$$

where L_s correspond to the number of symbols existing in one burst. The quantity $E\left[|e(f)|^2\right]$ is the Mean Square Error to be minimized.

The objective and design criteria for the canceller is to minimize the overall disturbance (MAI+noise) subject to the condition that $S^{(1)}(f)$ is not distorted. Therefore if for each frequency f and output band m we minimize the power spectral density of the disturbance, then the overall power is minimised and can be expressed as

$$C_m(f) = \left| G_{mB}^{(1)}(f) \right|^2 \left[L_s \sum_{u=2}^U \left| \sum_{i=-I}^I \left(\alpha_{i,m} \frac{G_{iB}^{(u)}(f)}{G_{iB}^{(1)}(f)} \right) \right|^2 + \sum_{i=-I}^I \left(|\alpha_{i,m}(f)|^2 \frac{\eta_{in_{iB}}(f)}{\left| G_{iB}^{(1)}(f) \right|^2} \right) \right] \quad (15)$$

This is equivalent to minimising the terms inside the rectangular brackets in (15) and consequently the optimum values of $\alpha_{i,m}$ are identical for each m , that is $\hat{\alpha}_{i,m} = \hat{\alpha}_i \quad \forall m$. Under these conditions we get

$$\begin{cases} \{\hat{\alpha}_i(f)\} = \arg \min_{\{\alpha_{i,m}(f)\}} [F_m(f)] \\ \sum_{i=-I}^I \alpha_{i,m}(f) = \text{rect}(fT) \end{cases} \quad (16)$$

where $F_m(f) = \frac{C_m(f)}{\left| G_{mB}^{(1)}(f) \right|^2}$.

Let us consider (16) for a particular f , where for simplicity of notation we drop the frequency variable in the different functions and the subscript m in the variables $\alpha_{i,m}$.

The function F in (16) can be represented by the Hermitian form

$$F(\{\alpha_i\}) = \boldsymbol{\alpha}^H \mathbf{H} \boldsymbol{\alpha} \quad (17)$$

The matrix \mathbf{H} is the Hessian Matrix (Appendix A) and $\boldsymbol{\alpha} = [\alpha_i]_{i \in \{-I, \dots, I\}}$.

The optimum weights $\{\alpha_i\}$ are found by the minimum of F with the restriction $\sum_{i=-I}^I \alpha_i(f) = 1$. Applying the method of Lagrange multipliers the minimum of F is found at

$$\boldsymbol{\alpha} = \mathbf{H} \mathbf{e}^{-1} \boldsymbol{\varphi} \quad (18)$$

where $\boldsymbol{\varphi}$ is a $2I + 1 \times 1$ vector with equal elements given by $1 / \sum_{l=1}^{2I+1} \sum_{c=1}^{2I+1} \text{He}_{l,c}^{-1}$ being $\text{He}_{l,c}^{-1}$ the element of line l^{th} and column c^{th} of the inverse of the Hessian.

The Hessian matrix is Hermitian definite positive (Appendix A) and it can be inverted through the Cholesky decomposition.

3.2 Multi-rate Generalization

Let us consider now the case of users with different spreading factors, which is of interest for UMTS-TDD. This standard was designed to accommodate multiple symbol rates by using different spreading factors. In the standard the spreading code is defined as the product between the channelization and the scrambling code. The channelisation code is used to spread a data symbol, whilst the scrambling code lasts for Q_{max} chips or during $\frac{Q_{max}}{Q}$ symbols where Q is the

spreading factor. Then to construct the spreading code, the channelization code must be repeated $\frac{Q_{max}}{Q}$ and multiplied by the scrambling code. The spreading code extends for more than one symbol when $Q \neq Q_{max}$.

The extension of the canceller to multi-rate can be easily performed by considering that a DS signal with spreading factor $Q = \frac{Q_{max}}{Z}$ can be decomposed as the sum of Z signals with spreading factor Q_{max} , where Z is a divisor of Q_{max} , and since in commercial systems as UMTS-TDD, Q_{max} is a power of two, then Z can be any power of 2 lower than Q_{max} .

The time domain representation of an information sequence using a spreading factor of Q is given by then

$$s(t) = \sum_{l=0}^{\frac{Q_{max}}{Q}-1} \sum_k a_k^l g_l \left(t - \frac{Q_{max}}{Q} kT \right) \quad (19)$$

where $\{a_k^l\}$ are the sequences of information symbols, $\frac{1}{T}$ the symbol rate and $g_l(t)$ the components of signature waveform. The components of the signature waveform at the receiver are given by

$$g_l(t) = \sum_{q=0}^{Q_{max}-1} c_q^l p(t - qT_c) * h(t) \quad (20)$$

where $p(t)$ is the normalized elementary pulse, $h(t)$ is a linear filter and $\{c_q^l\}_{q=0}^{Q_{max}-1}$ is given by

$$\{c_q^l\}_{q=0}^{Q_{max}-1} = \left(\underbrace{0, \dots, 0}_{Ql \text{ zeros}}, \tilde{c}_{Ql}, \dots, \tilde{c}_{Q(l+1)-1}, \underbrace{0, \dots, 0}_{Q_{max}-Q(l+1) \text{ zeros}} \right) \quad (21)$$

where $\{\tilde{c}_q\}_{q=0}^{Q_{max}-1}$ is the spreading sequence.

The composite signal at the receiver is given by

$$r(t) = \sum_{u=1}^U \sum_{l=0}^{\frac{Q_{max}}{Q_u}-1} \sum_k a_k^{l,u} g_l^{(u)} \left(t - \frac{Q_{max}}{Q_u} kT \right) + n(t) \quad (22)$$

where Q_u is the spreading factor of user u , and therefore assuming the information data sequences for each user consist of *i.i.d.* random variables, the signal of (22) can be interpreted as a composite signal consisting of $Z_U = \sum_{u=1}^U \frac{Q_{max}}{Q_u}$ DS-SS signals all of them with spreading factor of Q_{max} . Therefore the canceller will operate as the single rate case for a total of Z_U users where $Z_U \leq Q_{max}$.

4 Application of the Canceller to UMTS-TDD

To evaluate the canceller performance a simulation chain was implemented. Consisting of transmitters compliant with 3GPP specs of UMTS-TDD [15], a channel block and a multiuser receiver that can take several configurations. The processing is made in burst by burst basis and in the discrete domain. The channel parameters are assumed to be constant within each burst and assumed to be known.

The discrete impulse response of the channel for each burst is given by

$$w^{(u,a)}(n) = \sum_{l'=1}^L \alpha_{u,l',a} \gamma(\theta_{u,l'}; a) \delta_{kr} \left(n - \tau_{u,l',a} \right) \quad (23)$$

where $\alpha_{u,l',a}$ is the complex amplitude of the tap, $\tau_{u,l',a}$ is the delay of the tap in samples, δ_{kr} is the Kronecker impulse and $\gamma(\theta_{u,l'}; a)$ is in case of beamforming a complex amplitude of unitary modulus and phase dependent of the angle of arrival of the tap $\theta_{u,l'}$, on the geometry and antenna element of the array (24). The variable u is the index of the user, l' the index of the tap and a the index of the antenna. In beamforming configuration we drop the dependency on antenna a in $\alpha_{u,l',a}$ and $\tau_{u,l',a}$ because those parameters are equal in all antennas for the same user and tap. In the configurations with beamforming, the receptor sensor is a circular array of four antennas with 0.45λ spacing between elements (with 0.5λ arc between elements). In that case [16]

$$\gamma(\theta_{u,l'}; a) = e^{-j \frac{2\pi}{\lambda} R_c \cos(\theta_{u,l'} - \frac{2\pi(a-1)}{A})} \quad (24)$$

where A is the number of elements of the array, $a \in \{1, \dots, A\}$ is the index of the antenna, R_c is the radius of the antenna and λ is the wavelength. In space diversity, the antennas are spaced sufficiently apart that the channel of each other are uncorrelated. In that case $\gamma(\theta_{u,l'}; a) = 1$.

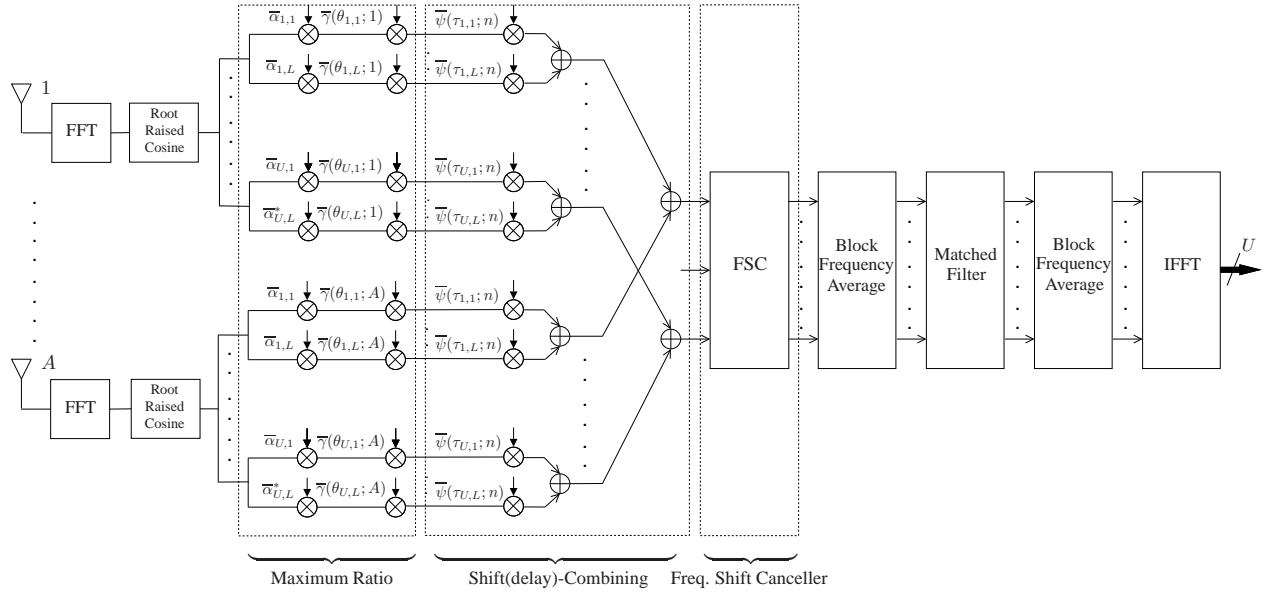


Figure 2: Configuration MaxRat-ShiftComb-FSC with multiple antennas and beam-forming.

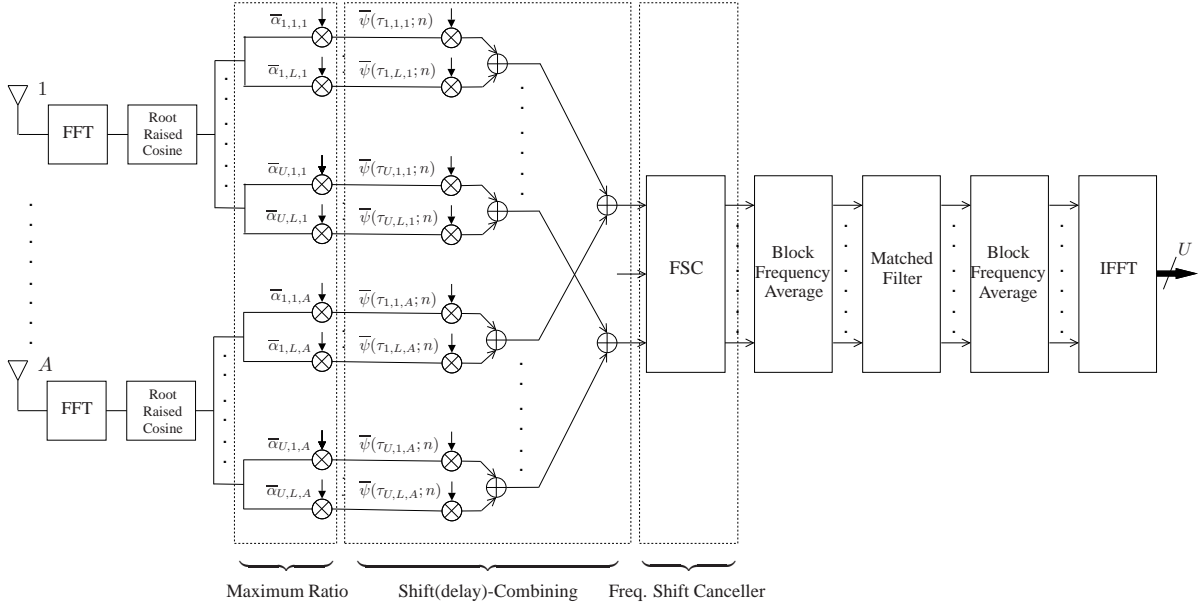


Figure 3: Configuration MaxRat-ShiftComb-FSC with multiple antennas and spatial diversity.

The corresponding channel frequency response is

$$W^{(u,a)}(n) = \sum_{l'=1}^L \alpha_{u,l',a} e^{-j2\pi\tau_{u,l',a}n/M} \gamma(\theta_{u,l'}; a) = \sum_{l'=1}^L \alpha_{u,l',a} \psi(\tau_{u,l',a}; n) \gamma(\theta_{u,l'}; a) \quad (25)$$

where M is the number of points of the FFT.

The channel model used in this work was the Geometrical Based Single Bounce Elliptical Model (GBSBEM) proposed by Liberti [17]. This model was developed for microcell and picocell environments. The propagation channel is characterized by one line of sight (LOS) tap and $L - 1$ taps for each user arriving from remote reflectors located randomly within an ellipsis where the base station and the mobile unit are at the foci.

The delay of each tap including the LOS tap is a random variable characterized by a probability density function whose expression can be found in [17]. After evaluating the delays of the taps, all LOS taps delays of all users are synchronized and the others shifted accordingly. The phase of the tap is uniformly distributed in $[0, 2\pi]$. The amplitude of the tap is obtained from a constant, dependent of the distance followed by the tap (it is proportional to $1/d_i^{p_l}$ where d_i is the distance and p_l is the pathloss exponent) and normalized (such that the sum of the power of all taps of that user is equal to one; in case of spatial diversity is equal to the number of antennas instead of one) times a random variable with

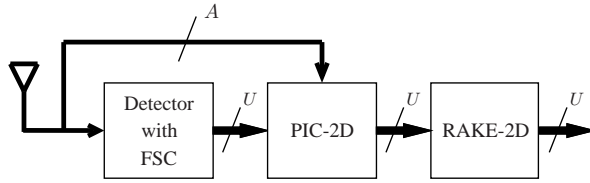


Figure 4: Receiver including FSC plus PIC-2D.

Table 1: Configurations simulated

Name	Operation Order			
	Unit 1	Unit 2	Unit 3	Unit 4
MaxRat-ShiftComb-FSC	Maximum Ratio	Shift(delay)-Combining	Freq. Shift Canceller	
MaxRat-FSC-ShiftComb	Maximum Ratio	Freq. Shift Canceller	Shift(delay)-Combining	
FSC-MaxRat-ShiftComb	Freq. Shift Canceller	Maximum Ratio	Shift(delay)-Combining	
MaxRat-ShiftComb-FSC+PIC	Maximum Ratio	Shift(delay)-Combining	Freq. Shift Canceller	PIC
MaxRat-FSC-ShiftComb+PIC	Maximum Ratio	Freq. Shift Canceller	Shift(delay)-Combining	PIC
FSC-MaxRat-ShiftComb+PIC	Freq. Shift Canceller	Maximum Ratio	Shift(delay)-Combining	PIC

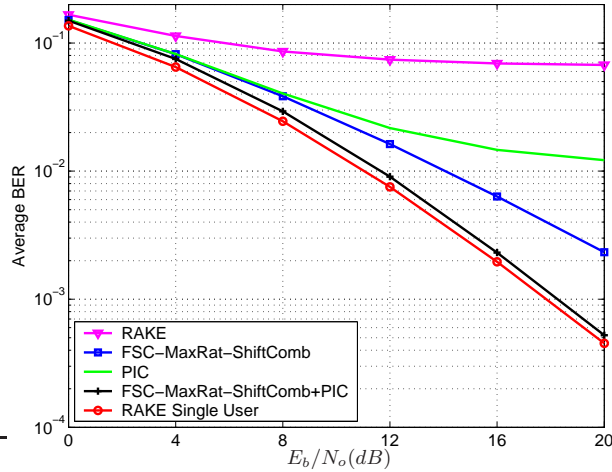


Figure 5: Single Antenna, UMTS-TDD System

Rayleigh distribution. The complex amplitude (amplitude and phase of the tap) is Doppler filtered.

In this model the angle of arrival (AOA) of the LOS tap of each user is fixed for one simulation and the angles of the other taps are random variables with mean equal to the AOA of LOS tap and a distribution given by [17]. Figures 2 and esquema2 each present a configuration including the FSC with beamforming and spatial diversity respectively. All other configurations presented in Table 1 are obtained by reordering the macro-blocks: Maximum Ratio, Shift(delay)-Combining and Frequency Shift Canceller

All configurations reduce to the RAKE-2D when the FSC operation is removed. In figures 2 and 3 the Block Frequency Average corresponds to a downsampling in time domain. The first downsampling factor is equal to the number of samples per chip, as the second downsampling aims to provide one sample per symbol and is thus equal to Q_{max} . So the length of the IFFT performed at the end of the chain is smaller than the FFT performed at the beginning. The transfer function of the matched filter is given by $FFT[\bar{\sigma}(\Delta - n)]$ [18] where $\bar{\sigma}(n)$ is the user spreading code (discrete). The constant Δ is such that $\bar{\sigma}(\Delta - n)$ is causal. The functions $\bar{\psi}(\tau_{u,l'}; n)$ and $\bar{\psi}(\tau_{u,l',a}; n)$ in Figures 2 and 3 respectively corresponds to a delay of $-\tau_{u,l'}$ and $-\tau_{u,l',a}$ in the time domain (Table 1).

Following (20) the FSC requires as parameters the discrete version of the linear response of the link up to its input, that is the concatenation of the channel impulse response, the root raised cosine filter and the blocks Maximum Ratio, Shift(delay)-Combining. For example for the configuration of Fig. 3 we get

$$h^{(b,u)}(n) = \sum_{a=1}^A \sum_{f=1}^F \sum_{l'=1}^L \alpha_{u,l',a} \bar{\alpha}_{b,f,a} \delta_{kr} \left(n - \tau_{u,l',a} + \tau_{b,f,a} \right) * Irrc(n) \quad (26)$$

Table 2: Simulation parameters settings

Redundant Bands	18
Number of Taps (per user and antenna)	2
Velocity	50 Km/h
Path Loss Exponent	3.7
Maximum Delay Spread	2.0 μ s
Number of samples per chip	4
Line of Sight Distance	300m
Number of Array Elements	4

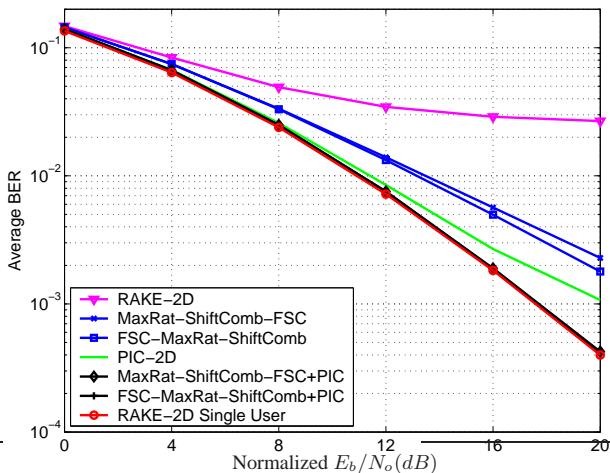


Figure 6: Beamforming, Circular Array, four antennas (A), UMTS-TDD System

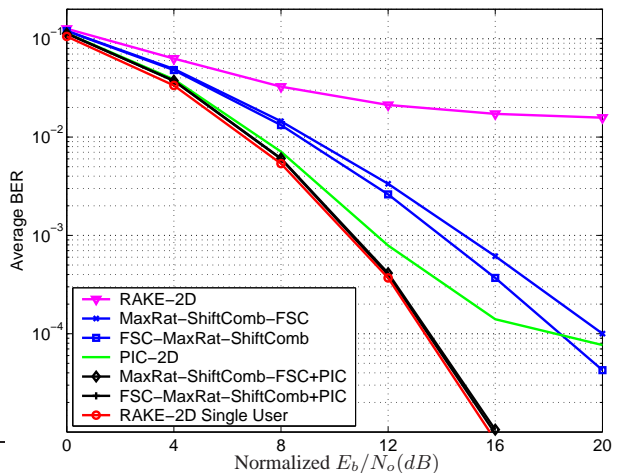


Figure 7: Spatial Diversity, four antennas (A), UMTS-TDD System

where b could take the values $b \in \{1, \dots, U\}$ representing each input burst in the FSC corresponding to each user to be recovered. Each burst have also signal components of all users. Each user in each burst is represented by $u \in \{1, \dots, U\}$. The letter L represents the number of taps of the transmission channel (for each user and antenna) and F represents the number of fingers of Maximum Ratio and Shift(delay)-Combining blocks (for each antenna and burst). In figure 3 $F = L$. The $Irrc(n)$ function is the impulse response of the root raised cosine. The discrete fourier transform of $h^{(b,u)}(n)$ is straight forward to calculate.

For configuration of figure 3 the power spectral density of the noise is given

$$\eta_{in}^{(b)} = \sum_{a=1}^A |W^{(b,a)}(n)|^2 |RRC(n)|^2 \eta^{(a)}(n) \quad (27)$$

where $\eta^{(a)}(n)$ is the power spectral density of noise in each antenna, $RRC(n)$ is the frequency domain root raised cosine and $W^{(b,a)}(n)$ is defined in (25). For the other cases the expressions equivalents to (26) and (27) can be easily derived.

The other detector configurations to be evaluated are the detectors with FSC concatenated with a single stage hard 2D-PIC (fig. 4). The reference configurations are the conventional 2D-RAKE and the conventional single stage 2D-PIC.

5 Simulation Results

In this section some numerical results are presented illustrating the performance of the proposed detector configurations with UMTS-TDD system and with time misalignment system. The simulations, whose results are presented in Figures 5, 6 and 7 were made with the parameters shown in Table 2 and considering the following scenario

- Number of users equal to eight, of which four use a spreading factor of 16, two a spreading factor of 8 and two a spreading factor of 4. This corresponds to a fully loaded system.
- The power assigned to each user is such that the Energy per Bit over the Spectral Density of Noise ($\frac{E_b}{N_0}$) is identical for all and therefore the power assigned to the users with spreading factor of eight and four is respectively 3 db and 6 db above the power assigned to the user with spreading factor of 16.

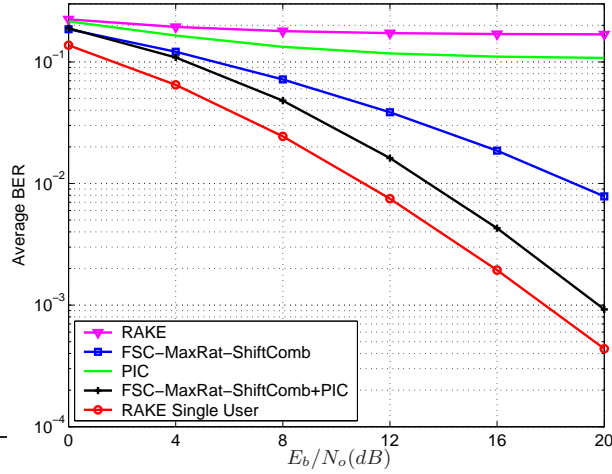


Figure 8: Single Antenna with time misalignment system

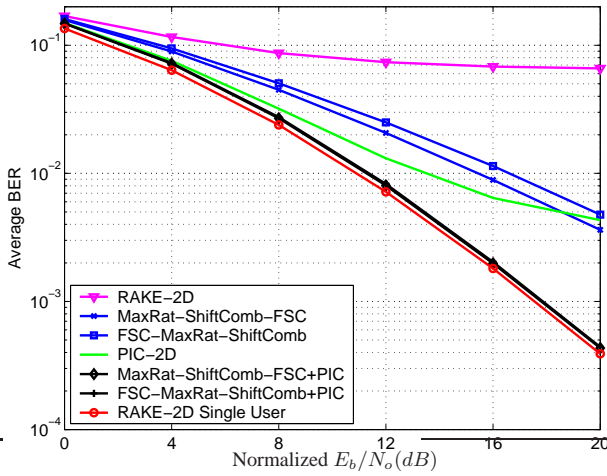


Figure 9: Beamforming, Circular Array, four antennas (A) with time misalignment system

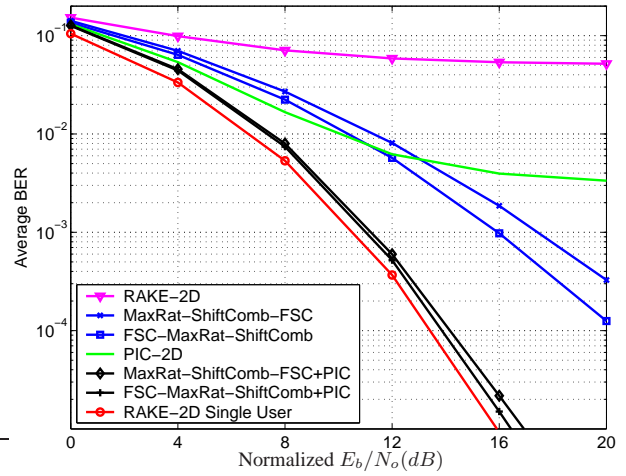


Figure 10: Spatial Diversity, four antennas (A) with time misalignment system

The results presented are only for the users with a spreading factor equal to 16. For the users with spreading factor of four the performance is slightly worst due interpath interference. The results of Fig. 6 and 7 are presented in terms of the normalized $\frac{E_b}{N_o}$ in dB, which is defined as the actual power efficiency minus the diversity antenna array gain $10\log_{10}A$ where A is the number of array elements. This is done to ensure that the algorithm is compared on a fair basis and to be able to separate the performance gains due to the algorithm and configuration from the gains due to the existence of diversity only.

For the single antenna case, all configurations exhibit the same performance. For the case of multi-element array the performance differs according to the relative positions of the Shift(delay)-Combining and FSC. Then the configurations FSC-MaxRat-ShiftComb and MaxRatFSC-ShiftComb have the same performance. Although the configuration MaxRat-ShiftComb-FSC gives the worst performance, in terms of complexity this configuration only needs $1/A$ the amount of matrix inversions in relation to the FSC-MaxRat-ShiftComb configuration (A is the number of antennas).

From Fig. 5, 6 and 7 we observe that either for the cases of beamforming or diversity, the use of the FSC provides considerable gains relatively to the 2D-RAKE and namely eliminates the bit error rate (BER) floor.

For the single antenna case the use of the FSC outperforms the PIC for moderate to high values of $\frac{E_b}{N_o}$. The same behavior is observed with multiple antennas but for higher values of $\frac{E_b}{N_o}$ (not shown in the plots of Fig. 6 e 7).

The use of the FSC with multiple antennas leads to gains compared to the single antenna case a 1.5 dB gain for a uncoded BER of 10^{-2} for the beamforming case, and up to 6 db for the diversity case.

The concatenation of the FSC and 2D-PIC detector nearly eliminates all the interference and the performance observed is almost coincident with the single-user 2D-RAKE performance.

In figures 8, 9 and 10 are presented the simulation results for system with time misalignment. In relation to synchronous system (UMTS-TDD), the channel profile for each user and burst suffers a delay with a uniform distribution from 0 to $1\mu s$.

As expected the results are worst than in UMTS-TDD system, but for multi-antenna scenario the performance approaches the 2D-RAKE single-user case.

6 Conclusions

In this paper we proposed a frequency domain, linear multiuser canceller able to operate with multi-rate signals. The canceller takes advantage of the frequency redundancy inherent in DS-SS signals, and the multi-rate extension was done by verifying that with UMTS-TDD like systems a signal with spreading factor which is a submultiple of the maximum spreading factor can be decomposed in several DS-SS signals each one with maximum spreading factor.

The performance of the canceller was evaluated for several configurations, either as a stand alone unit or concatenated with a PIC. The results have shown considerable improvements relatively to the 2D-RAKE, and with the application of multiple antennas in diversity case a considerable performance improvements was achieved. Furthermore when concatenated with a 2D-PIC, the performance achieved for both beamforming and diversity case is very close to the single-user bound and thus the FSC turns out to be a feasible candidate for interference cancellation and as a mean to provide clean signals to a low complexity PIC that can remove all the interference.

Acknowledgement

The authors would like to acknowledge Dr Cipriano Lomba and Dr Jonathan Rodriguez for their help in the preparation of the paper. This work was supported by a PhD Grant from PRAXIS XXI, Fundação para a Ciência e Tecnologia and the projects ASILUM and VISEF.

A Computation of the Gradient and Hessian

The function to be minimized in (16) is

$$F(\{\alpha_i\}_{i \in \{-I, \dots, I\}}) = L_s \sum_{u=2}^U \left| \sum_{i=-I}^I \left(\alpha_i \frac{G_{iB}^{(u)}}{G_{iB}^{(1)}} \right) \right|^2 + \sum_{i=-I}^I \left(|\alpha_i|^2 \frac{\eta_{in_{iB}}}{|G_{iB}^{(1)}|^2} \right) \quad (28)$$

Assume the following complex constant and positive real constant

$$Z_i^u = \frac{G_{iB}^{(u)}}{G_{iB}^{(1)}} \quad (29)$$

$$X_i = \frac{\eta_{in_{iB}}}{|G_{iB}^{(1)}|^2} \quad (30)$$

Given a complex function P then $|P|^2 = P\bar{P}$ (It could be identified such functions in (28)) then by inspection of (28) F is a real function dependent on the complex variables $\{\alpha_i\}$ and $\{\bar{\alpha}_i\}$. In this type of functions the stationary points could be taken by the gradient in relation to $\{\alpha_i\}$ or $\{\bar{\alpha}_i\}$ [19]. The gradient in relation to $\{\bar{\alpha}_i\}$ is preferable because the resultant gradient is dependant on the variables α_i .

It is given the following formula $\frac{\partial K(\{z_i, \bar{z}_i\}_i)}{\partial \bar{z}_k} = \frac{1}{2} \left[\frac{\partial K}{\partial x_k} + j \frac{\partial K}{\partial y_k} \right]$ where $z_k = x_k + jy_k$ [19] and K is a real function of complex variables.

Each element of the gradient vector is

$$\frac{\partial F(\{\alpha_i\}_{i \in \{-I, \dots, I\}})}{\partial \bar{\alpha}_k} = L_s \sum_{u=2}^U \left(\bar{Z}_k^u \sum_{i=-I}^I (Z_i^u \alpha_i) \right) + \alpha_k X_k \quad (31)$$

where the gradient vector is $\nabla F(\{\alpha_i\}_{i \in \{-I, \dots, I\}}) = \left[\frac{\partial F(\{\alpha_i\}_{i \in \{-I, \dots, I\}})}{\partial \bar{\alpha}_k} \right]_{k \in \{-I, \dots, I\}}$.

The Hessian Matrix is given by

$$\mathbf{H}_e = \left[\frac{\partial F(\{\alpha_i\}_{i \in \{-I, \dots, I\}})}{\partial \alpha_c \partial \bar{\alpha}_k} \right]_{k \in \{-I, \dots, I\}, c \in \{-I, \dots, I\}} \quad (32)$$

The coefficients of the Hessian Matrix are

$$\frac{\partial F(\{\alpha_i\}_{i \in \{-I, \dots, I\}})}{\partial \alpha_c \partial \bar{\alpha}_k} = L_s \sum_{u=2}^U Z_c^u \bar{Z}_k^u + X_k \quad c = k \quad (33)$$

and

$$\frac{\partial F(\{\alpha_i\}_{i \in \{-I, \dots, I\}})}{\partial \alpha_c \partial \bar{\alpha}_k} = L_s \sum_{u=2}^U Z_c^u \bar{Z}_k^u \quad c \neq k \quad (34)$$

The proof that the Hessian is positive definite is implied by the definition of Matrix positive definite. Then given the vector, $\mathbf{x} = [x_{-I}, \dots, x_0, \dots, x_I]^T$ the following inequality is always true for $\mathbf{x} \in \mathbb{C}^{2I+1}/\mathbf{0}$

$$[\mathbf{x}^H [\mathbf{H}\mathbf{e}] \mathbf{x}] = L_s \sum_{u=2}^U \left| \sum_{k=-I}^I x_k Z_k^u \right|^2 + \sum_{k=-I}^I X_k |x_k|^2 > 0 \quad (35)$$

when the superscript \mathbf{H} means transpose-conjugate. Then the matrix $\mathbf{H}\mathbf{e}$ is Hermitian definite positive and can be inverted by Cholesky decomposition. The Hessian matrix is Hermitian definite positive in all the domain of $\{\alpha_i\}$ and therefore the function F is strictly convex [20]. By the same process can be proved that the Hessian matrix of the function F with the restriction $\sum_{i=-I}^I \alpha_i(f) = 1$ (we proved only for F) is strict convex, and the minimum at (18) is global.

References

- [1] R. Kohno, R. Meidan, and L. B. Milstein, "Spread Spectrum Access Methods for Wireless Communications," *IEEE Communications Magazine*, vol. 33, pp. 58–67, January 1995. 1
- [2] S. Verdú, "Minimum Probability of Error for Asynchronous Gaussian Multiple-Access Channels," *IEEE Transactions of Information Theory*, vol. 32, pp. 85–96, January 1986. 1
- [3] Z. Xie, R. T. Short, and C. K. Rushforth, "A Family of Suboptimum Detectors for Coherent Multiuser Communications," *IEEE Journal of Selected Areas in Communications*, vol. 8, pp. 683–690, May 1990. 1
- [4] A. Klein and P. W. Baier, "Linear Unbiased Data Estimation in Mobile Radio Systems Applying CDMA," *IEEE Journal of Selected Areas in Communications*, vol. 11, pp. 1058–1066, September 1993. 1
- [5] A. Duel-Hallen, "A Family of Multiuser Decision-Feedback Detectors for Asynchronous Code-Division Multiple-Access Channels," *IEEE Transactions on Communications*, vol. 43, pp. 421–434, February/March/April 1995. 1
- [6] D. Guo, *Linear Parallel Interference Cancellation in CDMA*. M.Eng. Thesis, National University of Singapore, Dec. 1998. 1
- [7] D. Divsalar, M. K. Simon, and D. Raphaeli, "Improved Parallel Interference Cancellation for CDMA," *IEEE Transactions on Communications*, vol. 46, pp. 258–268, February 1998. 1
- [8] W. A. Gardner, *Cyclostationarity in Communications and Signal Processing*. IEEE PRESS, 1994. 1
- [9] W. A. Gardner, "Cyclic Wiener Filtering: Theory and Method," *IEEE Transactions on Communications*, vol. 41, pp. 151–163, January 1993. 1
- [10] J. Zhang, K. M. Wong, Z. Q. Luo, and P. C. Ching, "Blind Adaptative FRESH Filtering for Signal Extraction," *IEEE Transactions on Signal Processing*, vol. 47, pp. 1397–1402, May 1999. 1
- [11] J. Whitehead and F. Takawira, "Blind Adaptative Multiuser Detection for Periodically Time Varying Interference Suppression," in *IEEE Wireless Communication and Networking Conference*, (New Orleans, LA, USA), 13-17 March 2005. 1
- [12] J. H. Winters, "Smart Antennas for Wireless Systems," *IEEE Personal Communications*, vol. 5, pp. 23–27, February 1998. 2
- [13] L. C. Godara, "Applications of Antenna Arrays to Mobile Communications, Part I: Performance Improvement, Feasibility, and System Considerations," *Proceedings of IEEE*, vol. 85, pp. 1031–1060, July 1997. 2

- [14] H. C. Huang, *Combined Multipath Processing, Array Processing, and Multiuser Detection for DS-CDMA Channels*. Ph. D. Thesis, Faculty of Princeton, Princeton, USA, 1996. [2](#)
- [15] “3GPP TS 25.223,” *Spreading and modulation (TDD)*, Jan 2004. [5](#)
- [16] J. Litva and T. K.-Y. Lo, *Digital Beamforming in Wireless Communications*. Artech House Publishers, Boston, USA, First ed., 1996. [5](#)
- [17] J. C. Liberti and T. S. Rappaport, *Smart Antennas for Wireless Communications: IS-95 and Third Generation CDMA Applications*. Prentice Hall, New Jersey, USA, 1999. [6, 7](#)
- [18] G. L. Turim, “An Introduction to Matched Filters,” *IRE Transactions on Information Theory*, vol. 6, pp. 311–329, June 1960. [7](#)
- [19] B. A. D. H. Brandwood, “A Complex Gradient Operator and its Application in Adaptive Array Theory,” *IEE Proc., Pts. F and H*, vol. 130, pp. 11–16, February 1983. [10](#)
- [20] B. Pchénitchny and Y. Daniline, *Méthodes Numériques dans les Problèmes D’Extrémum*. Éditions MIR, Moscou, 1977. [11](#)